

EXPERIMENTAL EXAMINATION OF TYPE OF TILT MEASURED BY DIMM

B. S. Safonov¹

RESUMEN

DIMM es uno de los instrumentos más usados en la evaluación de sitios. Sin embargo, algunos aspectos de la medición de seeing con DIMM todavía son confusos; por ejemplo, qué tipo de inclinación DIMM mide en realidad – inclinación-g o inclinación-z? Diferencias en los resultados de estas dos opciones pueden ser tan grandes como 17% en la integral y 10% en seeing. Aquí se sugiere un método para determinar cuál inclinación se mide realmente por un instrumento dado y por el algoritmo para la determinación del centroide.

ABSTRACT

DIMM is one of the most used instrument in site testing. However some aspects of measuring seeing with DIMM still remain unclear, for example what kind of tilt DIMM actually measures – z-tilt or g-tilt? Difference in results for these two options can be as large as 17% in integral and 10% in seeing. Here we suggest a method to ascertain which tilt is actually measured by given instrument and centroiding algorithm.

Key Words: atmospheric effects — instrumentation: miscellaneous — site testing

1. INTRODUCTION

Differential Image Motion Monitor (DIMM) is a widely spread instrument for the measurement of seeing at astronomical sites. It is very robust and its theoretical description is quite transparent and well developed (Sarazin & Roddier 1990; Martin 1987). Though it was noted that DIMM observations suffer from several biases (Tokovinin 2002). In this paper we will consider one of these effects. The essence of this bias of interest is that dispersion of differential image motion depends not only on seeing but on how we measure the image position. There are two general models: to estimate the position of the photocenter of the image or the position of intensity maximum of image. The former way is realized when we estimate the position of the photocenter without thresholding (i.e., excluding pixels with intensity lower than certain fraction of maximal intensity). It corresponds to derivative of wavefront averaged over aperture. The latter situation starts to emerge when star is faint and we have to apply thresholding to improve accuracy of image position estimation. In this case we measure Zernike tip/tilt (Tokovinin 2002) because it is the parameter of wavefront that derives the position of intensity maximum.

The error in estimation of seeing due to improper suggestion about type of measured tilt can be as large as 10%. If we want to estimate the ground layer

intensity from difference between DIMM and MASS seeing, the error can become 30%. This is significant bias and it is especially important in cases of comparison of sites where different DIMMs with different image centroid algorithms was operated. Therefore for correct computation of seeing from dispersion we have to know what type of tilt we actually measure.

In this article we suggest to use ratio of longitudinal image motion dispersion to transversal one (hereafter LTR). As will be shown in § 2 this ratio also depends on type of tilt we measure. Unfortunately LTR also depends on distance of propagation of wavefront and finite exposure effects; we will consider these effects in § 2 either. Besides we will analyse the data obtained at SAI ASM installed on Mt. Shatdjatmaz (Kornilov et al. 2010) from this point of view (§ 3). Conclusion is given in § 4.

2. DIMM THEORY: EXPECTED LTR

In this section we will use the results described in report by V. Kornilov & B. Safonov². There we have shown that dispersion of differential image motion can be expressed as:

$$\sigma_{l,t}^{(g,z)2} = \int_0^\infty C_n^2(z) W_{l,t}^{(g,z)}(z) dz, \quad (1)$$

where $W_{l,t}^{(g,z)}$ is DIMM weighting function. It depends on device geometry, spectral characteristic, exposure and wind speed and direction. Letters g

¹Sternberg Astronomical Institute, Moscow State University, Universitetskii pr-t, 13, Moscow, Russia (safonov@sai.msu.ru).

²http://curl.sai.msu.ru/mass/download/doc/dimm_specs.pdf.

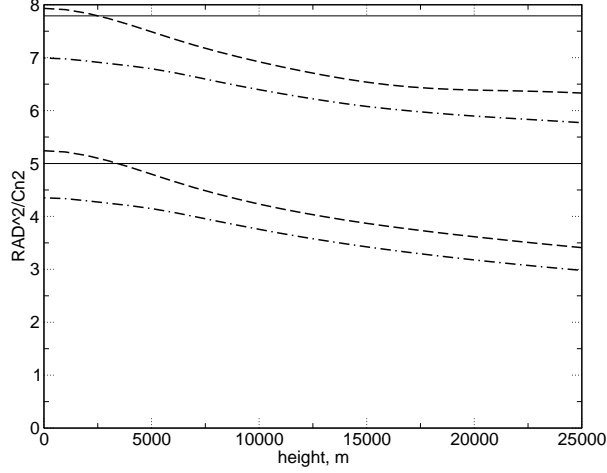


Fig. 1. Weighting functions for SAI DIMM (for parameters see text). Three upper lines correspond to longitudinal image motion, and three lower lines to transversal image motion. Dashed lines stand for z-tilt, dash-dot stand for g-tilt, thin horizontal lines correspond to simple formula by Sarazin & Roddier (1990).

and z indicate type of tilt we measure; l and t stands for longitudinal and transversal image motion, respectively. $C_n^2(z)$ is a turbulence profile. Weighting function by-turn:

$$W_{l,t}^{(g,z)} = \iint df_x df_y \Phi(f_x, f_y) F_{l,t}^{(g,z)}(f_x, f_y), \quad (2)$$

where $\Phi(f_x, f_y)$ is a spectral density of phase fluctuations for layer with $C_n^2(h)\Delta h = 1$; $F_{l,t}(f_x, f_y)^{(g,z)}$ is spectral filter of DIMM. Spectral filter is a product of several filters, two of them are of special interest for us, let's extract them:

$$F_{l,t}^{(g,z)}(f_x, f_y) = G_{l,t}^{(g,z)}(f_x, f_y) \cos(\pi\lambda z f^2) \text{sinc}(\tau V f_x), \quad (3)$$

where $\cos(\pi\lambda z f^2)$ is responsible for the dependence of weighting function on altitude, $\text{sinc}(\tau V f_x)$ describes dispersion attenuation due to finite exposure time τ (V is wind speed). We have to note that this expression is valid for the case of monochromatic radiation. For the finite passband the propagation term $\cos(\pi\lambda z f^2)$ will transform into more complex expression, for details see report by Kornilov & Saonov.

Weighting functions computed for SAI DIMM device are shown in Figure 1. SAI DIMM have the following parameters: diameter of subapertures $D = 90$ mm, distance between centers of apertures $B = 196$ mm, exposure time $\tau = 4$ ms. It can be seen that DIMM response depends on turbulence altitude quite significantly. Propagation also affects

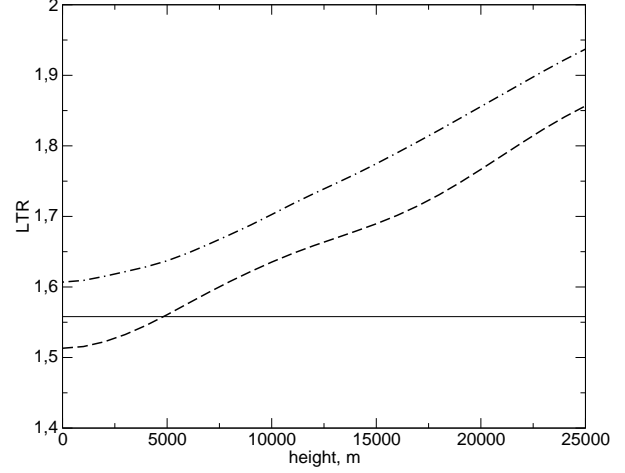


Fig. 2. LTR dependence on altitude. Ratio of weighting function for longitudinal motion to transversal one. Dashed line stands for z-tilt, dash-dot stands for g-tilt, thin horizontal line corresponds to simple formula from Sarazin & Roddier (1990).

the LTR; the Figure 2 illustrates this fact. Fortunately MASS/DIMM data can be reduced for this effect because MASS gives the information about high-altitude atmospheric layers intensities (similar procedure was applied in Kornilov et al. 2010).

3. COMPARISON WITH OBSERVATIONAL DATA

3.1. DIMM Data used for analysis

As we already have mentioned the type of tilt we measure is defined basically by centroiding algorithm. In our case it consists of window and thresholding. In process of windowing we exclude all pixels outside the circular window of radius of 7 pixels ($\approx 3.5\lambda/D$ for our device) centered on brightest pixel. For computation of photocenter position we consider only pixels with intensity greater than $3\sigma_B + B$, where B is background and σ_B its error. We compute dispersions of photocenter position for longitudinal and transversal image motion for 2 sec periods and then average them on 1 min intervals. Also for purposes of this article we don't correct measurements for the finite exposure time, we will consider this effect separately later.

For analysis we will use the data obtained with DIMM channel of SAI MASS/DIMM device (Kornilov et al. 2010) in period 2007–2009. We have filtered these data according to the following criteria to minimize influence of respective undesirable effects on LTR:

1. Several periods of not properly aligned instrument was excluded (18.7% of data).

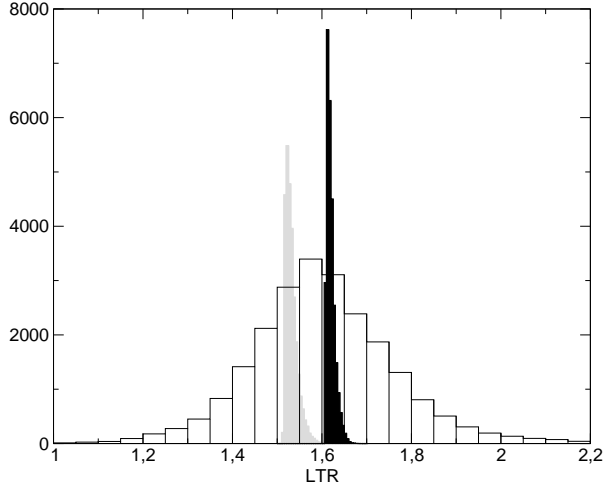


Fig. 3. Distribution of LTR. Grey distribution stands for LTR expected from profile in assumption of z-tilt, black for g-tilt, clear for observed distribution of LTR.

2. Flux < 40000 . DIMM CCD has no sufficient dynamical range for measurement of the brightest stars. So we excluded respective observations to avoid problems with non-linearity.

3. Airmass < 1.3 . Some fraction of observations was made at high airmasses (for atmospheric extinction estimation).

Filtered data accounts for 59.3% of total amount.

3.2. Dependence on altitude

Thanks to the presence of MASS data we are able to take into account propagation term in the integrand in the left part of the equation (3) and to compute the *expected* value of LTR for each data point. In the Figure 3 one can see these distributions for the case of z-tilt and g-tilt. First of all it can be seen that the propagation term doesn't affect the LTR much, respective distributions are quite narrow. This is especially noticeable against the background of distribution of actually observed LTR which is also presented in this figure. This can be explained by the fact that LTR is a ratio of two random numbers with χ^2 distribution with ≈ 30 degrees of freedom.

But in the first place we interested in means of these distributions: for expected values of LTR for z- and g-tilts and observed values of LTR it amounts for 1.532, 1.620 and 1.603, respectively. So observed values of LTR lies between values predicted in assumptions of z- and g-tilts. Anyway we cannot say anything without the consideration of the effect of finite exposure time. We will do this in the next section.

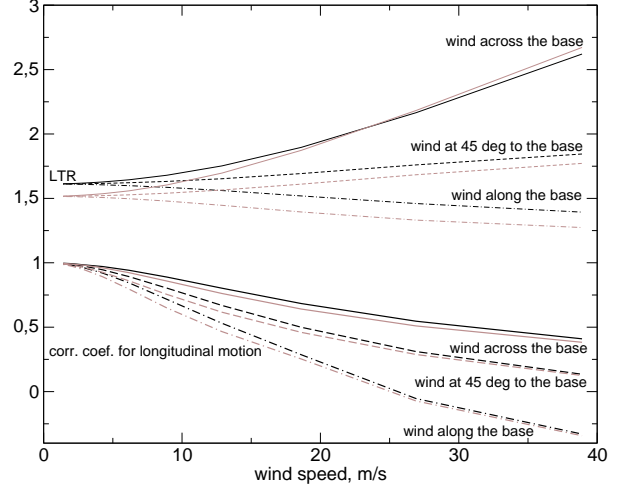


Fig. 4. Dependence of LTR (upper 6 curves) and correlation coefficient of longitudinal differential image motion (lower 6 curves) on wind speed (see the text for details). Black lines computed for g-tilt, grey for z-tilt. Solid lines stand for wind blowing across the base, dashed for wind blowing at 45° degrees to the base and dash-dot for wind blowing along the base.

3.3. Dependence on wind speed

As we mentioned before the effect of propagation on LTR is quite small and can be neglected for purposes of this subsection because as we will see soon the effect of finite exposure time is much greater. We computed it for parameters of our device, results displayed in Figure 4. One can see that LTR depends on wind speed greatly and moreover it also depends on wind *direction* respective to the base, what can lead to the widening of LTR distribution. Unfortunately we cannot directly compare this graphs with experimental data because we have no reliable data on wind speed and direction. Instead we will use the correlation coefficient between consequent estimations of centroid position r as a measure of wind speed. The behaviour of r as a function of wind speed was evaluated by means of theory already used in § 2, results is represented in Figure 4. It is important that it monotonically decreases with wind speed.

The dependence of LTR (upper 6 curves) on correlation coefficient of longitudinal differential image motion and observational data is represented in Figure 5. It can be clearly seen that for high r observed LTR can be described quite well in assumption of z-tilt. For lower r the situation become more complex due to the fact that ranges of LTR predicted by theory for z- and g-tilt start to overlap. Because

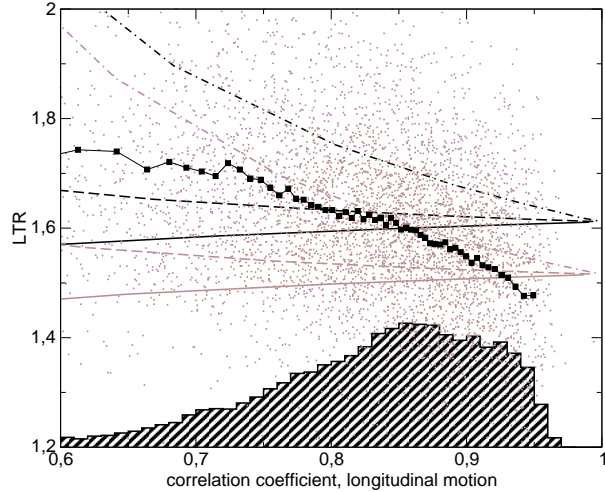


Fig. 5. Dependence of LTR (upper 6 curves) on correlation coefficient of longitudinal differential image motion. Meaning of lines are the same as on Figure 4. Grey points indicate observational data (every tenth point displayed). In lower part of graph the distribution of correlation coefficient is represented.

of it we cannot say anything for sure for correlation coefficients $r < 0.85$.

4. SUMMARY

In this paper we have recalled a problems with proper interpretation of basic DIMM observable – dispersion of differential image motion. It was shown that wrong assumptions about measurement process (type of tilt we measure) can lead to significant bias in measurement of turbulence characteristics. For example if we use the formula deduced under assumption of g-tilt while our device measures z-tilt, that can lead to overestimation of 10% for seeing and up to 30% for ground layer intensity.

We have suggested the ratio of longitudinal to transversal image motion dispersion (LTR) as an indicator of type of tilt we measure. Properties of this indicator was investigated by means of DIMM spectral filter theory (propagation and finite exposure time was considered). For SAI DIMM it was shown that at least at low wind speed situation, i.e. when correlation coefficient of longitudinal image motion between consequent frames $r < 0.85$, what can be explained under assumption of z-tilt.

This work can be continued in the following directions:

- Changing parameters of centroid algorithm will allow us to check how measured values of dispersions depend on them.
- Propagation of light in turbulent atmosphere, process of image formation and procedure of measurements can be numerically simulated. By means of such simulation we can directly ascertain what we actually measure. This option is also less model-dependent, in other words it would allow us to consider other possible models of centroid position estimation apart from g- or z-tilt.

I would like to thank my scientific supervisor Dr. Victor Kornilov for valuable discussions. Experimental data used for analysis was obtained on SAI ASM station which was constructed and being operated by SAI site testing team: V. Kornilov, N. Shatsky, O. Voziakova, S. Potanin, & M. Kornilov.

REFERENCES

- Kornilov, V., Shatsky, N., Voziakova, O., Safonov, B., Potanin, S., & Kornilov, M. 2010, MNRAS, 408, 1233
 Martin, H. M. 1987, PASP, 99, 1360
 Sarazin, M., & Roddier, F. 1990, A&A, 227, 294
 Tokovinin, A. 2002, PASP, 114, 1156

